Electronic Supplementary Material (ESI) for Journal of Materials Chemistry C.

Supplementary material: Implications of acceptor doping in the polarization and electrocaloric response of $0.9Pb(Mg_{1/3}Nb_{2/3})O_3–0.1PbTiO_3$ relaxor ferroelectric

Andraž Bradeško,[a] Marko Vrabelj,[a] Lovro Fulanović,[a] Šarūnas Svirskas,[b] Maksim Ivanov,[b] Ringaile Katiliūte,[b] Džiugas Jablonskas,[b] Mantas Šimėnas,[b] Gediminas Usevičius,[b] Barbara Malič,[a,c] Juras Banys,[b] Tadej Rojac,[a,c,*]

[a] *Jožef Stefan Institute, Jamova cesta 39, 1000 Ljubljana, Slovenia*
[b] *Faculty of Physics, Vilnius University, Saulėtekio al. 9, 10222 Vilnius, Lithuania*
[c] *Jožef Stefan International Postgraduate School, Jamova cesta 39, 1000 Ljubljana, Slovenia*
**Corresponding author at: Electronic Ceramics Department, Jožef Stefan Institute, Jamova cesta 39, 1000*

1. Powder properties

X-ray diffraction (XRD) patterns of Undoped, Mn-0.5 and Mn-1.0 powders after mechanochemical treatment of the initial powder mixture are shown in Fig. S1. Only the perovskite phase is detected in the powders (JCPDS 81-0861), confirming a successful mechanochemical reaction leading to the perovskite formation.

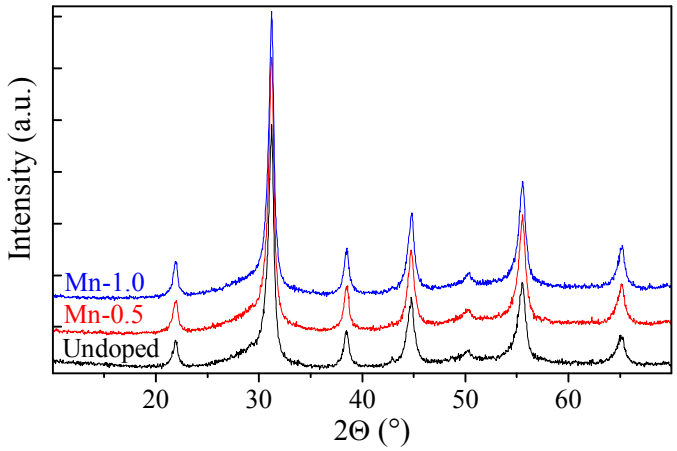

Fig. S1. XRD patterns of the Undoped, Mn-0.5 and Mn-1.0 ceramic powders after mechanochemical treatment of the initial oxide mixture. (JCPDS 81-0861)

The average particle size and particle size distribution histograms of the powders after mechanochemical treatment, determined by a light-scattering technique (Microtrac S3500), are shown in the Fig. S2. Fine, mostly submicron powders are produced in all cases with similar average particle size.

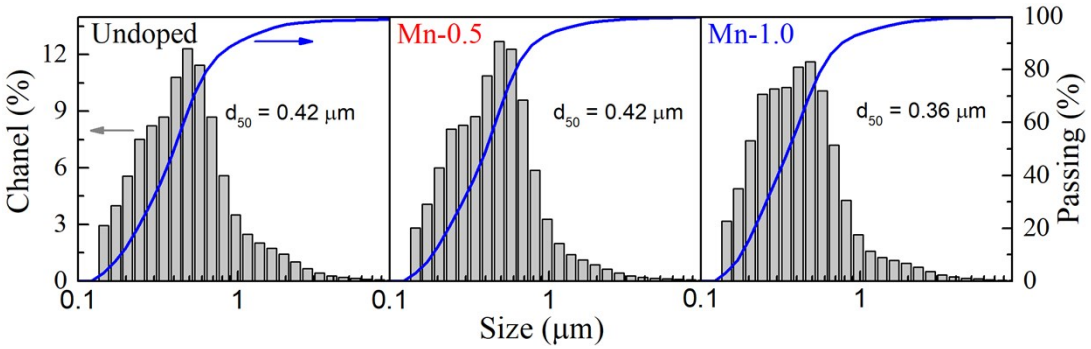

Fig. S2. Particle size distribution of the Undoped, Mn-0.5 and Mn-1.0 powders, prepared by mechanochemical synthesis.

2. Dynamic sintering curves

The dynamic sintering curves of Undoped, Mn-0.5 and Mn-1.0 powder compacts reveal different shrinkage behaviour of the doped samples, compared to undoped (Fig. S3) Both Mn-0.5 and Mn-1.0 samples start to shrink at a lower temperature (~670°C) than the undoped sample (~950°), implying on the presence of the liquid phase in the Mn-doped samples. All the samples shrank until the melting point at ~1320 °C [1].

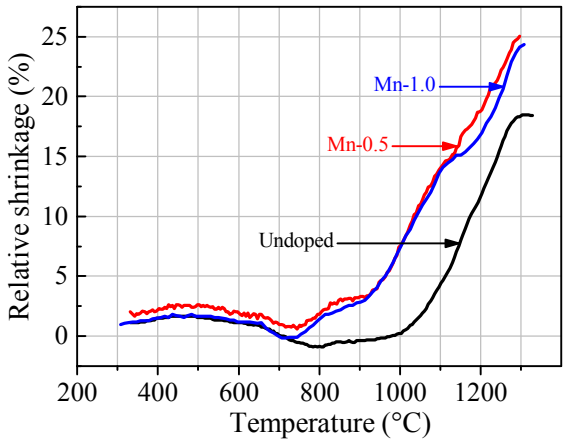

Fig. S3. The dynamic sintering curves of Undoped, Mn-0.5 and Mn-1.0 powder compacts.

3. Sintered ceramics

The XRD patterns of undoped, Mn-0.5 and Mn-1.0 ceramic samples are shown in Fig. S4. The reflections in the XRD pattern of the crushed samples correspond to the perovskite phase only (JCDPS 81-0861), irrespective of the Mn-addition. Detrimental pyrochlore phase, which displays a maximum reflection at ~29.2° was not detected (see the inset in Fig. S4).

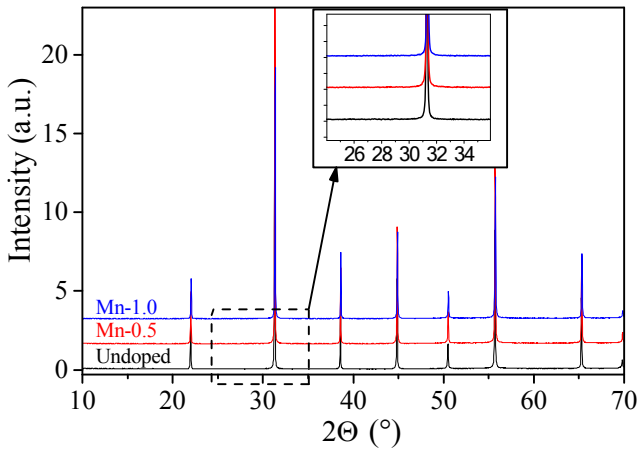

Fig. S4. XRD patterns of undoped and doped PMN-PT ceramics (crushed pellets).

Fig. S5 and S6 show the microstructural analysis of the undoped and doped PMN-PT ceramic samples. The scanning electron microscopy (SEM) images of the etched surfaces (Fig. S5a-c) reveal dense microstructures, in agreement with the measured relative densities, which were in the range 95 %–97 % (see next figure, Fig. S6). The undoped and Mn-1.0 samples have comparable average grain size, i.e., 4.1 ± 2.1 µm and 4.7 ± 2.5 µm, respectively, while, the average grain size of Mn-0.5 ceramics is smaller, 3.0 ± 1.5 µm (Fig. S6). Prepared samples have unimodal grain size distribution, indicating predominantly normal grain growth (Fig. S6).

A detailed FE-SEM analysis of the Undoped sample confirmed clean grain boundaries without segregation of secondary phases (Fig. S5d); however, a discontinued intergranular glassy phase was found in the Mn-0.5 and Mn-1.0 samples (Fig. S5e,f). The thickness of the intergranular phase in Mn-1.0 sample is approximately 100 ± 20 nm with little variations in the thickness either along the length of individual boundaries or throughout the sample. Further FE-SEM investigations showed that in Mn-0.5 only a minor part of grain boundaries contains glassy phase (boundaries are predominantly clean) while in Mn-1.0 a larger fraction of boundaries contains this phase. Note that the glassy phase was found in the fractured surfaces but not in the polished ones, indicating that this phase is possibly removed by the polishing process. According to the energy-dispersive X-ray spectroscopy (EDXS) analysis of the fractured surfaces of the Mn-1.0 sample, the intergranular phase is rich in Pb and Mn. The presence of the glassy phase is in a good agreement with the dynamic sintering curves of the doped powder compacts with the shrinkage onset occurring at low temperatures, compared to the undoped sample (see Fig. S3 and associated discussion).

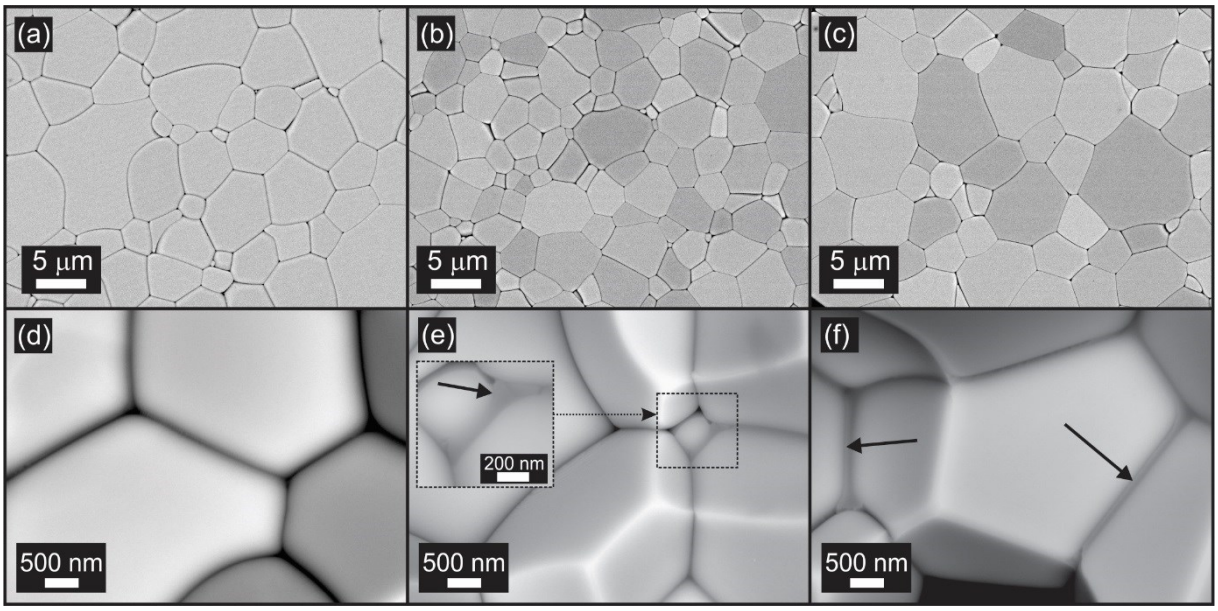

Fig. S5. SEM micrographs of the etched surfaces of (a) Undoped, (b) Mn-0.5 and (c) Mn-1.0 samples. FE-SEM micrographs of the fractured samples of (d) Undoped, (e) Mn-0.5 and (f) Mn-1.0 samples. Solid arrows indicate intergranular glassy phase rich in Pb and Mn (according to EDXS analysis; see text for details).

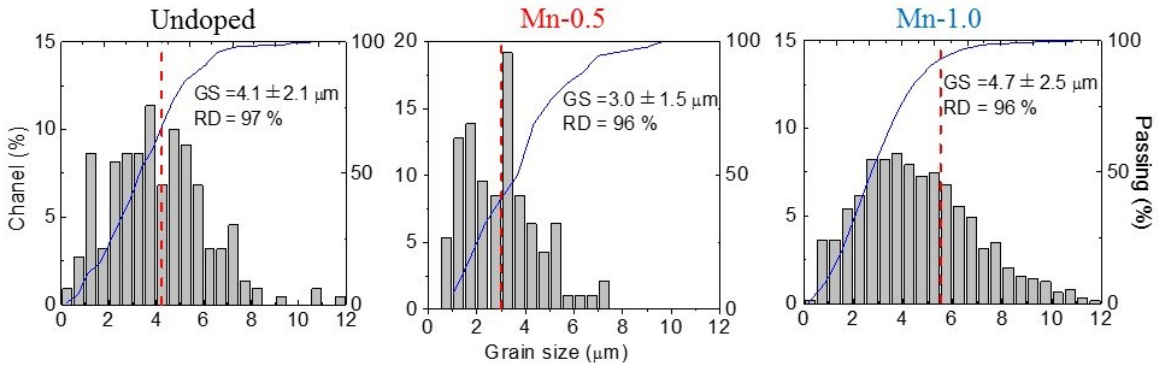

Fig. S6. Grain size distributions together with the cumulative curve for the Undoped, Mn-0.5 and Mn-1.0 ceramics. The average grain sizes (GS; *also denoted with a vertical dashed line) and relative densities (RD) are added on the histograms.*

4. Temperature dependent EPR spectroscopy

Figure S7 shows the EPR spectra of the PMN-10PT samples doped with 0.5% Mn collected at different temperatures. The EPR line shape is qualitatively the same at all temperatures, indicating that the chemical Mn environment does not change in a broad temperature range even by crossing the freezing point (which corresponds to the peaks in the pyroelectric signals; see main paper Figure 3).

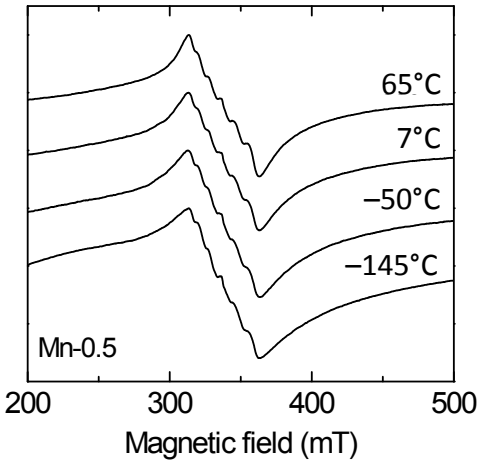

Fig. S7. Temperature dependent X-band EPR spectrum of PMN-10PT doped with 0.5% Mn.

5. Temperature dependent nonlinear dielectric response

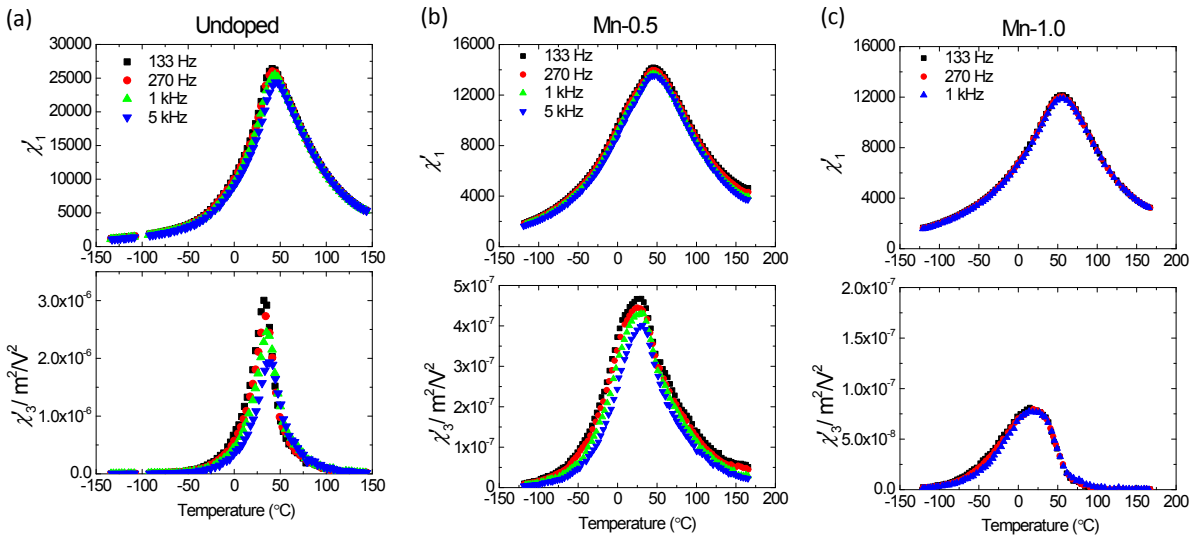

Fig. S8. Temperature dependence of the 1st (upper plot) and 3rd order susceptibility (lower plot) of (a) undoped, (b) Mn-0.5 and (c) Mn-1.0 PMN-10PT samples. Note the different vertical scales.